Astron. Astrophys. 317, 25–35 (1997)

ASTRONOMY AND ASTROPHYSICS

Soft X-ray properties of the narrow line QSO Ton S180 k (RX J0057.3–2222)

H.H. Fink[1], **R. Walter**[2,3], **N. Schartel**[4], **and D. Engels**[5]

[1] Max-Planck-Institut für extraterrestrische Physik, D-85748 Garching bei München, Germany
[2] *INTEGRAL* Science Data Centre, Chemin d'Écogia 16, CH-1290 Versoix, Switzerland
[3] Observatoire de Geneve, Chemin des Maillettes 51, CH-1290 Sauverny, Switzerland
[4] ESA, IUE Observatory, Vilspa, P.O.Box 50727, E-28080 Madrid, Spain
[5] Hamburger Sternwarte, Universität Hamburg, Gojenbergsweg 112, D-21029 Hamburg, Germany

Received 8 March 1996 / Accepted 14 May 1996

Abstract. Close to the celestial position of the QSO Ton S180 a bright X-ray source was detected by ROSAT during the all-sky survey. Pointed follow-up observations confirmed the positional coincidence of RX J0057.3–2222 and Ton S180. The X-ray radiation of the quasar is intensity variable on time scales of hours to days and years with amplitudes up to a factor of about two. During the observation in June 1992 an outburst of the X-ray emission occurred with a rise time of less than one day and a decay extending possibly over weeks. These intensity variations are not accompanied by corresponding spectral changes. On the other hand, a clear change of the quasar's spectrum was observed for the time interval between two observations separated by 23 days without noticeable intensity variations. For most observations the measured count rate spectrum of the QSO in the soft (0.1 - 2.4)keV energy band is best represented by a two-component spectrum consisting of a power law with a photon index $\Gamma = 3.10$ and a steep low energy component for which we choose a black body spectrum. Its temperature is unusually low, $kT \approx 16$eV, causing this component to be dominant below 0.3 keV. During the observed spectral change the power law component flattens ($\Gamma = 2.79$) and the low energy component vanishes. The low energy absorption obtained from the fit is inconsistently larger than the absorption due to cold matter in our Galaxy. Although intrinsic absorption by cold matter is therefore probable, there are no signs in the residuals of the spectral fits indicating the existence of ionized matter on the line of sight. With its variable X-ray emission and its steep soft spectrum the narrow line QSO Ton S180 shares the typical X-ray properties of the class of narrow line Seyfert 1 galaxies.

Key words: galaxies: active – galaxies: Seyfert – galaxies: quasars individual Ton S180 - X-rays: general

Send offprint requests to: H.H. Fink, MPE address

1. Introduction

In the First *Extreme Ultraviolet Explorer* Source Catalogue (Bowyer et al., 1994) the bright EUV source EUVE J0057-223 was identified with the UV-excess object KUV 00549-2239 of the Second Kiso Catalogue (Kondo, Noguchi, and Maehara, 1984). Bowyer et al.(1994) classified this object as a white dwarf. A close inspection of the sky field around KUV 00549-2239 (Hamuy, Maza, 1989; Bowen et al., 1994) revealed that the UV object is actually identical with the bright emission line object Ton S180 (Wisotzki et al., 1995).

Ton S180 is an optically bright galaxy with a Seyfert 1 spectrum (V=14.4) (Veròn-Cetty, 1984; Chavira, 1958) showing quite narrow permitted lines (FWHM = 900 km/s) and strong FeII emission. These features classify Ton S180 as a narrow line Seyfert 1 object (Boller, Brandt, Fink, 1995). With a redshift of z = 0.06198 (Wisotzki et al., 1995) its absolute magnitude is $M_B = -23.1$ ($H_o = 50$ km/s Mpc; $q_o = 0$) qualifying the object as a QSO (Schmidt, Green, 1986). *UBVRI* photometry of Ton S180 revealed the quasar to be slightly variable with amplitudes of the order of 0.1 mag (Veròn-Cetty, 1984; Hamuy, Maza, 1987; Winkler, 1992). EUV flux measurements of EUVE J0057-223 reported by Vennes et al. (1995) yielded a flux density of $\nu F_\nu = 3.9 \cdot 10^{-11}$ erg cm^{-2} s^{-1} at $\nu = 3.4 \cdot 10^{16}$ Hz (0.14 keV) assuming a power law continuum with a photon index of $\Gamma = 2.4$ and Galactic absorption $N_H = 1.6\ 10^{20}$ cm^{-2}. In addition, there are indications of large amplitude EUV variability. The ROSAT observations with their superb photon statistics are the first X-ray measurements of the narrow line QSO Ton S180.

2. Observations and data analysis

The X-ray source RX J0057.3–2222 was repeatedly observed with the XRT/PSPC telescope (Aschenbach, 1988; Pfeffermann et al., 1987) aboard the ROSAT satellite (Trümper 1983): once during the all-sky survey (RASS) in 1990 (Thomas et al., 1991)

Table 1. Observation log

Year	Date	Observation ROSAT Observation ID	No. of Data Subset	Begin UT	X-Ray Data Exposure [s]	Source Counts	CountRate* [cts/s]
a) ROSAT All-Sky Survey							
1990	16-18 Dec	RASS		21:27:16	610	989	1.62 ± 0.05
b) ROSAT Pointed Observations							
1992	18 June	701139P	1	14:41:57	1370	4592	3.35 ± 0.05
		701140P	2	16:18:57	1553	5201	3.33 ± 0.05
	19 June	701141P	3	16:13:57	1536	10382	6.75 ± 0.06
			4	17:50:57	1532	8995	5.87 ± 0.06
	28 June	701142P	5	12:11:42	1444	7227	5.00 ± 0.06
			6	13:48:42	1504	8490	5.64 ± 0.06
	18 Dec	701139P-1	7	00:23:23	1396	4876	3.49 ± 0.05
			8	01:03:52	1422	5346	3.76 ± 0.05
1993	10 Jan	701140P-1	9	02:00:02	1700	6772	3.98 ± 0.05
	16 June	701451P	10	07:12:44	1054	3390	3.22 ± 0.06
			11	08:48:43	575	1757	3.06 ± 0.07
			12	10:23:25	664	1633	2.46 ± 0.06
		701452P	13	11:59:37	726	2056	2.83 ± 0.06
			14	13:35:37	868	2753	3.17 ± 0.06
			15	15:09:49	1694	5566	3.29 ± 0.04

* vignetting and deadtime corrected

and several times during pointed observations at four occasions in 1992 and 1993. The detailed observation log is given in Table 1 together with the exposure and the registered source strength for each individual observation. The listed X-ray data refer to ROSAT's energy band (0.1 - 2.4)keV. The total exposure, spread over two and a half years, is 19648 s, during which more than 80.000 counts were accumulated.

The celestial positions of the X-ray source as derived from the centroids of its X-ray images are (α_{2000} = $00^h57^m20^s.0$ $\delta_{2000} = -22^o22'52"$) for the RASS observation and ($\alpha_{2000} = 00^h57^m19^s.8$ $\delta_{2000} = -22^o22'54"$) for the merged pointed observations. The most precise measurement ($\pm 0".5$) of the optical position of Ton S 180 found in literature are the Kiso coordinates ($\alpha_{2000} = 00^h57^m19^s.9$ $\delta_{2000} = -22^o22'59".2$) (Kondo, Noguchi, and Maehara, 1984). The deviation of $7".2$ between the optical and the RASS X-ray position is well within the 90% confidence error circle of 32" radius (Fig.1), which was determined for the positions of survey sources by comparison with optical star catalogues (Voges, 1992). The 90% confidence error circle for the merged pointed observations, also given in Fig. 1, comprises a statistical error of $2".6$ resulting from a maximum likelihood source detection algorithm and an intrinsic uncertainty of 6" of the attitude solution. In order to establish the X-ray data sets for the temporal and spectral analysis, the image of the source was extracted from the X-ray image of the sky field scanned by the telescope during the survey or viewed in pointed observations. The image reconstruction of the X-ray sky was achieved using the attitude solution. Each registered X-ray count was corrected for vignetting according to the off-axis angle of its impact point onto the PSPC. The extraction radius was chosen according to radial profiles of the point source's image. It is 2' in the RASS case and 3' for the brighter images of the pointed observations. For the RASS observation the background level was determined from two circular fields,

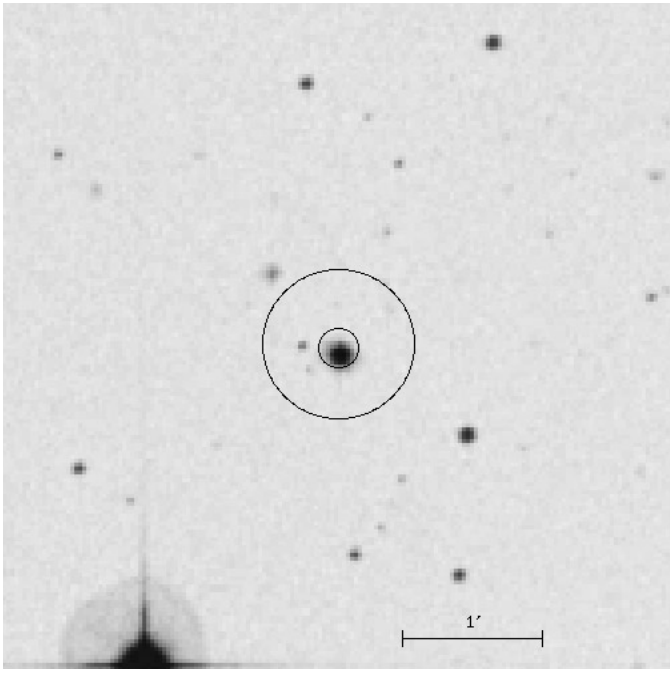

Fig. 1. Sky field around Ton S 180 taken from the Digitized UK Schmidt Sky Survey. In addition, the 90% confidence error circles of the X-ray positions from the RASS (large circle) and from the merged ROSAT pointed observations (small circle) are shown. (Copyright 1993, 1994, Association of Universities for Research in Astronomy Inc.)

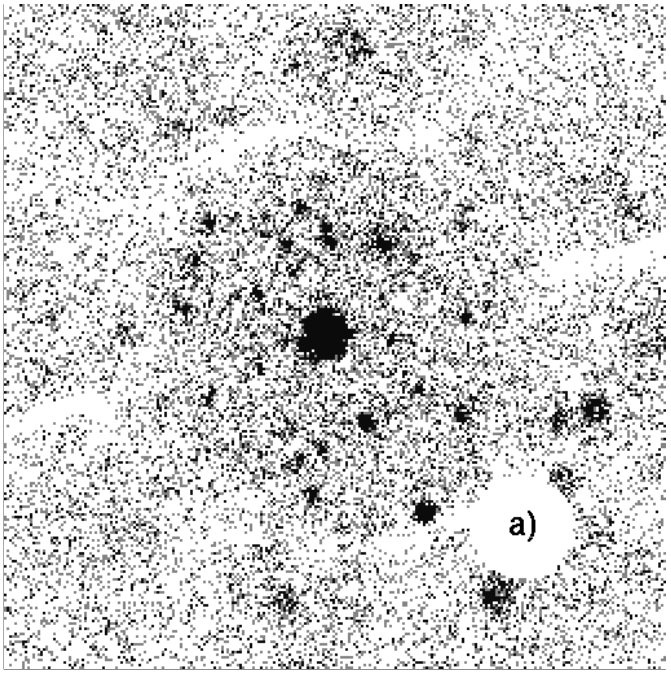

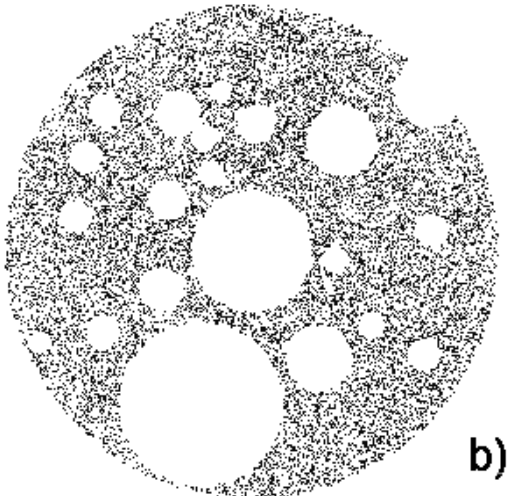

Fig. 2a and b. X-ray image of RX J0057.3–2222 and its surroundings and the background field. **a** central part of the field of view with the target source near the center. **b** geometry of the sky field used to determine the X-ray background in the vinicity of the target source.

free of sources and located on the scan path near the target object. The survey background surface brightness amounted to $9 \cdot 10^{-4}$ cts s^{-1} arcmin^{-2}.

The X-ray data of the pointed observations consist of 15 subsets (Table 1) corresponding to 15 individual ROSAT orbits with a typical target exposure of about 1500 s. To obtain a reliable background field, we merged the sub sets to a total X-ray image. Its central part is reproduced in Fig. 2a. As can be seen from the picture, the target source RX J0057.3–2222 (Ton S180), located near the center of the field of view (FOV), is surrounded by numerous other X-ray sources. In addition, the shadow of the central annular supporting structure of the PSPC's entrance window is faintly visible in the X-ray image. To avoid this affecting of the image analysis, a circular sky field with a radius of 19' was cut out from the central FOV. Subsequently, this image field was subjected to a maximum likelihood source detection algorithm to identify all X-ray sources which were detected with a likelihood of more than 10. In total, 27 X-ray sources were detected and removed from this image section. After extracting the target source, the geometry of a background field was obtained as shown in Fig. 2b. In analyzing the individual data sets of each orbit this background geometry was always applied. The mean background surface brightness of the pointed observations as derived from the merged data set is $1.4 \cdot 10^{-3}$ cts s^{-1} arcmin^{-2}. With reference to the source extraction area (28.27 arcmin^2) the mean background rate is therefore ≈ 0.04 cts/s, about a factor of hundred lower than the mean source count rate corrected for instrumental effects (vignetting and dead time corrections).

3. X-ray light curves

The number of source counts accumulated during the 1.7 days of the ROSAT survey observation is too small to allow the construction of a statistically significant survey X-ray light curve. Therefore, we restrict the study of the X-ray variability of Ton S180 to the pointed observations in 1992 and 1993.

In order to prevent that the X-ray image is shaded accidentally by the wires of the PSPC entrance window supporting grids, the telescope axis is wobbled with a period of 400s and an amplitude of 3' (Briel, 1991), while the telescope is pointed at a target source. This causes the source's image to move across the wires, averaging out the obscuration effects. In reconstructing a stable X-ray image the wobble is removed *a posteriori* by applying the attitude solution. As the pointing of the telescope is actively controlled by the Attitude Measurement and Control System of the satellite, an attitude jitter is superimposed on the linear wobble movement. Consequently, the point source image performs a random walk over the detector along the wobble path, which makes the actual shading of the image by the supporting grids unpredictable. A reliable intensity estimation of the point source image can therefore only be obtained by averaging the count rate over an entire wobble period. Nevertheless, different wobble pathes cause different averaged count rates, but the variation of the flux determination in the wobble mode is less than 4% (Hasinger, private communication). As a consequence of the wobble mode, the smallest time scale reproducibly measurable with the PSPC in pointed observations is 400s.

The QSO was observed at four epochs, each separated by about half a year. As can be seen from Table 1, the pointed observations in June 1992 comprise six orbits which are grouped to three pairs of adjacent orbits separated by one and by eight and a half days, respectively. The second observational epoch in Dec 1992 consists of two adjacent orbits. The first observation in 1993 lasting only one orbit took place 23 days later. In June 1993 the QSO was observed during six successive orbits.

The intra-orbit variability of the source is determined by splitting up the total exposure per orbit into 400s bins, starting with the arrival time of the first incident photon. Usually, the

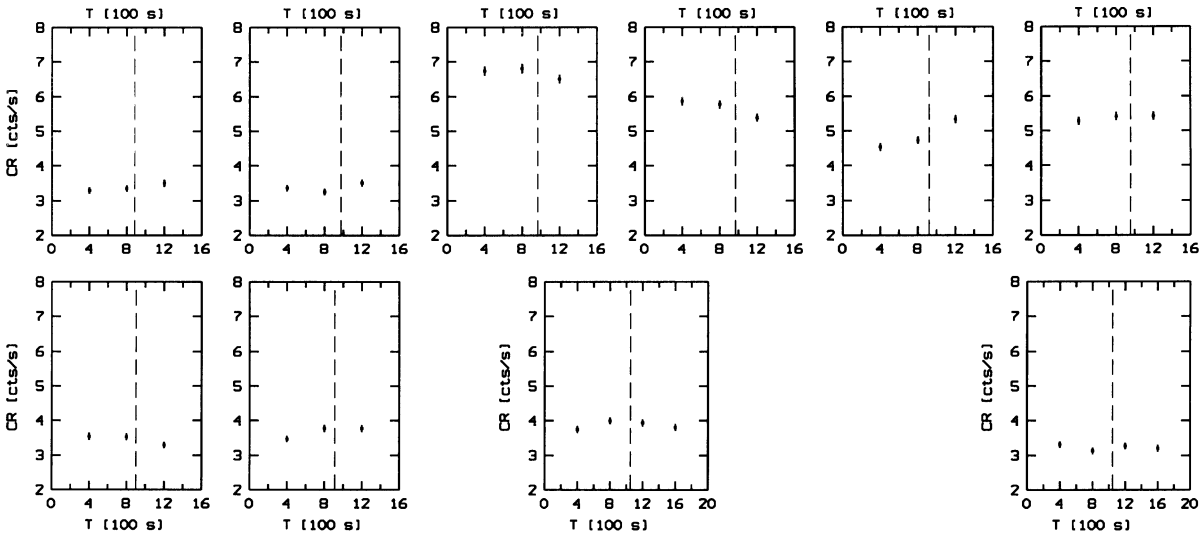

Fig. 3. Intra-orbit X-ray light curves of pointed observations in 1992 and 1993. The upper panel shows the six orbits in June 1992. The first two diagrams of the lower panel refer to the Dec observation in 1992 and the third diagram shows the light curve of the one orbit observation in Jan. 1993. The last light curve corresponds to the last pointing of the June 1993 observations. The dashed lines indicate the midpoints of the observations as given in the orbit-to-orbit lights curves in Fig. 4

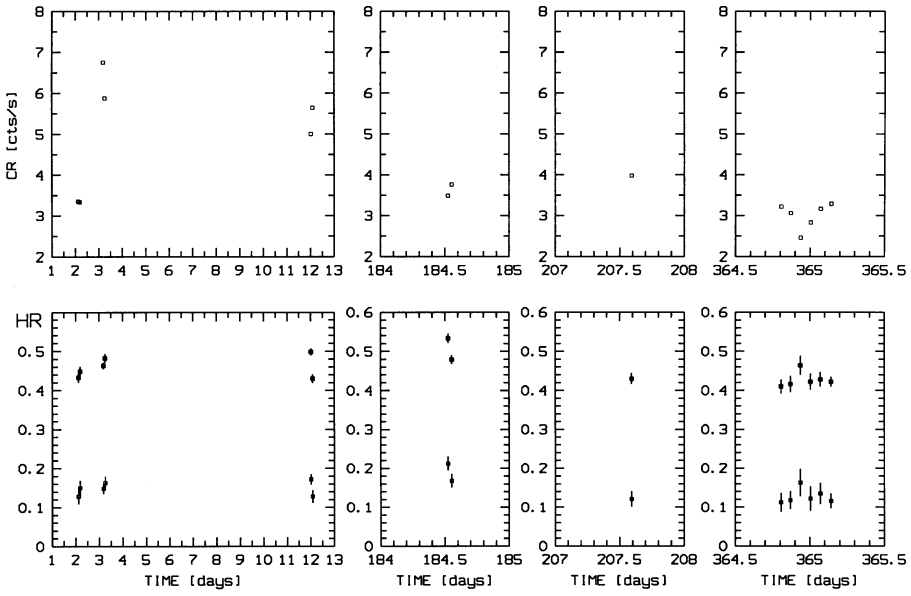

Fig. 4. X-ray light curves of Ton S180 and hardness ratios. Upper panel: Orbit-to-orbit light curve of the observations in 1992 and 1993. The error bars of the data points are smaller than the symbol size. Columns from left to right: June 1992, Dec. 1992, Jan. 1993, June 1993. The co-ordinate axis labeled TIME starts with the Julian Date 2448790.0. Lower panel: Hardness ratios in the carbon window of the PSPC entrance window's transmission Lower data points: hardness ratio HR1; upper data points: hardness ratio HR2 (for definitions see text)

exposure per orbit is not an integer multiple of 400s. The incomplete last bin has to be rejected for the purpose of contructing a light curve, because the averaging over an uncomplete wobble period would yield unreliable count rates. For the count rate per 400s bin all vignetting corrected counts within the source extraction area are gathered which are registered within the time limits of the bin considered. The source count rate per bin is obtained by subtracting the extrapolated background count rate referring to the source extraction area. Finally, a dead time correction has to be applied which is mainly determined by the master veto anti-coincidence rate.

All of the observations in 1992 contain three 400s bins, whereas the 1993 observations are shorter with the exception of that one in January and of the last pointing in June which contain four 400s bins. The intra-orbit light curves of those observations comprising three or more 400s bins are shown in Fig. 3. Obviously, the count rate varies smoothly over the orbits. There are no "noisy" orbits such as those found in the case of the BL Lac object PKS 2155-304 (Brinkmann et al., 1994). The maximum intra-orbit variation occurs in the fifth orbit of the June 1992 observation. There the count rate varies by 18% over three bins corresponding to a formal doubling time of 0.08 days.

The orbit-to-orbit X-ray light curves of Ton S180 are given in the upper panel of Fig. 4. The data points are obtained by summing up the count rates of the 400s bins and by dividing the sum by the integer multiple of 400s contained in the orbit exposure.

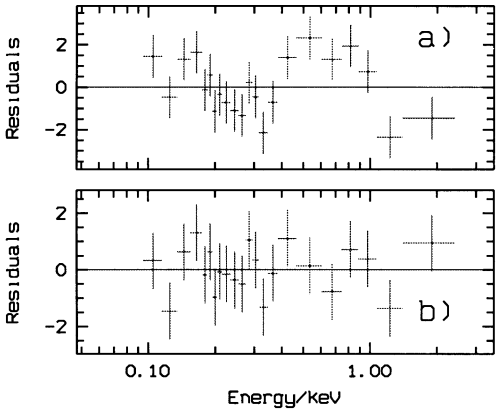

Fig. 5a and b. Residuals of the best fits. **a** simple power law, **b** power law plus black body component. The low energy absorption is a free fit parameter

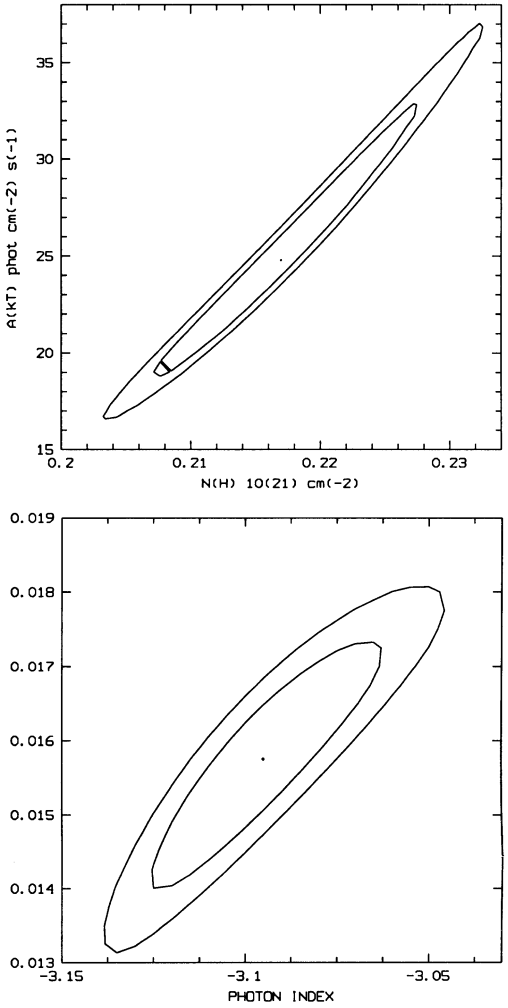

Fig. 6. Significance contours of the fit parameters. The contours of the 68.3% and the 90% confidence levels are given for two interesting parameters.

In June, 1992, the (0.1 - 2.4)keV count rate rises from a level of 3.34 cts/s in the first two orbits to 6.75 cts/s almost one day later. The upper limit of the corresponding doubling time is 0.99 days. In the following orbit the count rate drops by 13% corresponding to a negative doubling time of 0.52 days. Eight and a half days later the source is found to emit at a mean count rate level of 5.2 cts/s. The undersampling of the light curve does not allow to state definitely that the decay time of the outburst in orbit No.3 is much longer (days to weeks) as the rise time (1 day).

During the two orbits in Dec 1992 the source emits at a count rate level of about 3.6 cts/s and does not vary significantly. 23 days later in Jan, 1993, the source is found at a slightly higher count rate level of 4 cts/s, but, again, the intra-orbit variations are negligible.

During the observation in mid 1993 the count rate drops from a level, which equals almost that one the 1992 June observation started with, by 31% over three orbits and rises again to the initial level in three further orbits. The formal doubling time of this variation is 0.64 days.

Finally it should be noted that the mean count rate of Ton S180 during the survey observation, 1.62 cts/s, is lower by a factor of two than the mean rate during the pointed observations. Therefore, the amplitude of the long-term variability of Ton S180 is quite as large as that one of the orbit-to-orbit variations with a time scale of one and a half hour.

In the lower panel of Fig. 4 the hardness ratios HR1 = (CR(0.1−0.2)keV−CR(0.5−2.4)keV)/CR(0.1−2.4)keV and that one of the entire carbon window of the PSPC's transmission, HR2 = (CR(0.1 − 0.29)keV − CR(0.5 − 2.4)keV)/CR(0.1 − 2.4)keV, are shown. If we exclude orbit-to-orbit variations of the quasar's spectrum as unrealistic, there are no signs of remarkable spectral variability in the June observations in 1992 and 1993, respectively. On the other hand, the hardness ratios measured in Dec 1992, $< \text{HR1} >= 1.900 \pm 0.025$, and in Jan 1993, HR1 = 1.210 ± 0.020, have inconsistent values, even if we adopt appreciably higher uncertainties, possibly indicated by the putative variability of adjacent orbits, as the pure statistical errors given.

4. Soft X-ray spectra

In order to establish soft X-ray spectra in the energy range (0.1 - 2.4)keV for all data sets, the vignetting corrected photon events accumulated from the source extraction area were sorted into 256 pulse height channels to yield the source plus background count rate spectrum. The same procedure is performed for the background counts gathered from an off-source sky field and renormalized to the source extraction area. After subtracting the background spectrum and employing the dead time correction, a binned up pulse height source count rate spectrum, corrected for instrumental effects, is obtained. It is used to compare it with *a priori* defined model spectra by means of least squares fit procedures which use that detector response matrix valid for the time of observation.

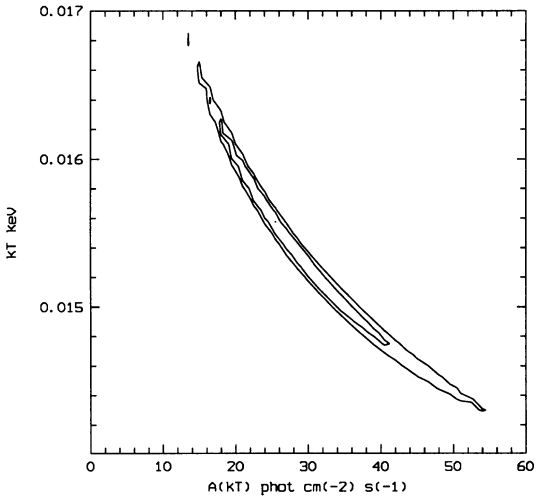

Fig. 7. Statistical characteristics of the low energy component dominating the spectrum of Ton S180 below 0.3 keV. The contours of the 68.3% and the 90% confidence level are given for two interesting parameters

4.1. The mean spectrum

To get an idea of the shape of the quasar's soft X-ray spectrum we decided to merge those data sets of the pointed observations, for which the hardness ratio in Fig. 4 does not indicate a spectral change, i.e. we merged all data sets of the June observations in 1992 and 1993. The extracted source and background counts of the merged orbits were accumulated and processed as described above. The resulting mean count rate spectrum of Ton S180 contained 63.000 cts registered in 15130s.

Firstly, we fit a simple power law modified by low energy absorption to the source spectrum. Thereby we restrict the fit to data between channel 10 ($\sim$ 0.1 keV) and channel 240 ($\sim$ 2.4 keV) as beyond these boundaries the detector response matrix is not well defined. The channel spectrum was then compressed to 22 spectral bins with an equal significance of their count contents. In the case of the mean spectrum the significance per spectral bin was 47 standard deviations. The simple power law fit with the absorption as a free parameter proved to be unacceptable. The best fit parameters were: photon index $\Gamma = 2.91 \pm 0.03$, normalization at 1 keV $A_{PL} = (4.21 \pm 0.08)10^{-3}$ phot cm^{-2} s^{-1} keV^{-1}, and cold matter absorption $N_H = (1.32 \pm 0.06)10^{20}$ cm^{-2}. The minimum reduced χ^2 of the fit was 38.5/19 d.o.f. = 2.03. The errors given correspond to one standard deviation (68.3% confidence level) for three interesting parameters. The residuals between the actual count rate spectrum and the model spectrum are depicted in Fig. 5a showing systematic trends troughout the spectral range. The N_H-value as resulting from the fit was inconsistently lower than the Galactic value towards Ton S180, $N_{Hgal} = 1.48 \cdot 10^{20}$ cm^{-2} (Stark et al., 1992), even at a 90% confidence level. This might indicate the existence of an additional spectral component at very low photon energies. Fixing N_H to the Galactic value worsens the fit even more.

An appreciable improvement is achieved by fitting a two-component model spectrum consisting of a power law, a black body, and cold matter absorption. The fit of this model to the merged data yielded the following parameters: $\Gamma = 3.10 \pm 0.05$, $A_{PL}(1keV) = (4.30 \pm 0.08)10^{-3}$ phot cm^{-2} s^{-1} keV^{-1}, $kT = 15.7 \pm 2.5$ eV, $A_{kT} = 24 \pm 10$ phot cm^{-2} s^{-1}, and $N_H = (2.15 \pm 0.15)10^{20}$ cm^{-2}. The goodness of fit is given by a reduced χ^2-value of 14.3/17 d.o.f. = 0.84. The improved residuals are reproduced in Fig. 5b. The fit reveals that the black body component dominates the quasar's count rate spectrum below 0.3 keV. The remaining range between 0.1 keV, the low energy limit of the spectrum due to absorption essentially in our Galaxy, and 0.3 keV is too narrow to determine the exact spectral shape of the additional low energy component. Therefore, the actual choice of its spectral shape is rather arbitrary. The fit is effectively not changed by substituting the black body by thermal bremsstrahlung or by a second steep power law.

The N_H-value resulting from the fit is at a 90% confidence level inconsistently larger than the Galactic value towards Ton S180. This might be due to a small amount of intrinsic absorption in the host galaxy of the QSO or in its nuclear region. It is further remarkable that the fit temperature of the black body component is unusually low compared to the spectra of Seyfert 1 galaxies showing soft X-ray excesses (Walter & Fink, 1993; Walter et al., 1994).

For the assessment of the statistical interdependence and significance of the spectral parameters resulting from the fit we studied the significance diagrams of the mutually dependent parameter pairs (Γ, kT) and (N_H, A_{kT}). The corresponding significance contour diagrams are given in Fig. 6. As expected, the parameters (Γ, kT), which determine the shape of the continuum and which are dominant in different energy bands, are less mutually dependent. They show narrow error ranges and their values are well defined. This is not the case for (N_H, A_{kT}), the significance contours of which are shown in Fig. 6a. The interplay of the exponential low energy cut-off due to absorption by interstellar matter and the strength of the steep energy component of the intrinsic quasar spectrum determines the rise of the observed count rate spectrum below 0.2 keV. Since the low energy component is dominant only below 0.3 keV, the interdependence of both parameters is very strong. Consequently, the χ^2-valley is extended and shallow causing particularly the strength of the steep component to be poorly defined. This effect is further increased for the fits of the orbit spectra discussed in the next section, which contain many fewer counts than the merged spectrum.

Fig. 7 summarizes the statistical characteristics of the low energy spectral component and illustrates how poorly the normalization of the black body can be determined, while its temperature is well defined.

4.2. Orbit spectra

As the hardness ratio given in Fig. 4 indicates the possibility of a slight change of the quasar's spectrum between Dec 1992 and Jan 1993, we wished to investigate the spectral parameters as a

Table 2. Fits of the orbit spectra

a) Simple Power Law

No. of data subset	Significance[a] per spectral bin	A_{PL}[b] 10^{-3} $phot/cm^2\ s\ keV$	Γ	N_H $10^{20}\ cm^{-2}$	${\chi^2}_{min}/19$
RASS	5.9	3.02 ± 0.45	3.12 ± 0.18	1.94 ± 0.65	0.53
1	12.4	3.53 ± 0.23	2.84 ± 0.13	1.29 ± 0.23	0.89
2	13.2	3.27 ± 0.21	2.82 ± 0.11	1.14 ± 0.21	1.30
3	19.2	6.37 ± 0.29	3.01 ± 0.08	1.45 ± 0.16	1.06
4	17.6	5.16 ± 0.26	3.04 ± 0.09	1.40 ± 0.17	0.86
5	17.3	4.25 ± 0.25	3.08 ± 0.10	1.42 ± 0.19	0.55
6	17.3	5.74 ± 0.28	2.97 ± 0.09	1.50 ± 0.19	0.99
7	13.0	2.62 ± 0.20	3.03 ± 0.13	1.12 ± 0.20	1.13
8	13.5	3.32 ± 0.22	3.01 ± 0.12	1.34 ± 0.22	1.11
9	15.0	$4,27 \pm 0.23$	2.75 ± 0.10	1.15 ± 0.17	0.83
10	10.8	3.53 ± 0.26	2.81 ± 0.15	1.31 ± 0.27	1.19
11	7.6	3.33 ± 0.35	2.78 ± 0.19	1.25 ± 0.36	1.14
12	7.3	2.47 ± 0.28	2.63 ± 0.18	0.82 ± 0.31	1.49
13	8.5	3.01 ± 0.30	2.81 ± 0.18	1.25 ± 0.33	0.43
14	9.6	3.40 ± 0.29	2.72 ± 0.15	1.08 ± 0.27	0.58
15	14.1	3.45 ± 0.20	2.83 ± 0.11	1.26 ± 0.20	0.73

b) Power Law + Black Body

No. of data subset	A_{PL}[b] 10^{-3} $phot/cm^2\ s\ keV$	Γ	A_{kT} $phot/cm^2\ s$	kT eV	N_H $10^{20}\ cm^{-2}$	${\chi^2}_{min}/17$
RASS	3.10 ± 0.47	3.21 ± 0.22	5^{+25}_{-5}	18.4 ± 2.5	$2.7^{+1.9}_{-0.7}$	0.59
1	3.55 ± 0.14	2.92 ± 0.15	16^{+117}_{-14}	13.0 ± 2.6	1.60 ± 0.73	0.96
2	3.33 ± 0.14	3.06 ± 0.16	71^{+74}_{-36}	13.2 ± 3.4	2.01 ± 0.80	1.19
3	6.75 ± 0.32	3.24 ± 0.15	138^{+148}_{-88}	17.0 ± 2.8	3.32 ± 0.36	1.00
4	5.20 ± 0.17	3.17 ± 0.15	460^{+223}_{-317}	10.7 ± 3.4	1.82 ± 0.62	0.66
5	4.31 ± 0.20	3.23 ± 0.16	14^{+157}_{-2}	16.6 ± 4.0	2.12 ± 0.72	0.54
6	5.79 ± 0.16	3.16 ± 0.11	1802^{+1861}_{-1663}	10.0 ± 5.8	2.10 ± 0.43	0.78
7	2.68 ± 0.18	3.33 ± 0.17	160^{+158}_{-88}	13.1 ± 2.6	2.25 ± 0.67	0.92
8	3.35 ± 0.23	3.19 ± 0.14	55^{+57}_{-36}	13.4 ± 1.1	1.99 ± 0.48	0.95
9	4.28 ± 0.19	2.79 ± 0.11	4^{+31}_{-4}	$13.3^{+3.0}_{-13.3}$	1.26 ± 0.30	0.91
10	3.71 ± 0.22	3.21 ± 0.20	300^{+900}_{-250}	13.8 ± 4.2	3.12 ± 1.05	0.91
11	3.65 ± 0.21	3.22 ± 0.24	1400^{+2450}_{-1120}	13.9 ± 5.1	4.28 ± 1.10	0.70
12	2.68 ± 0.27	2.94 ± 0.32	220^{+360}_{-200}	14.9 ± 5.2	3.48 ± 1.15	1.59
13	3.19 ± 0.31	3.07 ± 0.30	66^{+391}_{-53}	16.5 ± 4.8	3.19 ± 2.71	0.43
14	3.50 ± 0.20	2.99 ± 0.21	64^{+186}_{-42}	13.9 ± 5.6	2.15 ± 1.21	0.49
15	3.73 ± 0.24	3.10 ± 0.19	231^{+955}_{-201}	16.0 ± 3.6	3.48 ± 1.85	0.65

a The PHA spectra are compressed to 22 spectral bins. Significance in units of standard deviations.
[b] at 1 keV

function of time in more detail. All subsets of data, RASS and the individual orbits of the pointed observations, comprise enough counts to allow the construction of statistically significant X-ray spectra.

Again, we firstly fit the orbit spectra with a simple absorbed power law. Due to the poorer statistics the representation of the orbit spectra by simple power laws cannot be rejected in all fits as in the case of the mean spectrum. More than half of the fits was revealed to be statistically acceptable. Considering one standard deviation as error, the mean index of the observations in June 1992, $< \Gamma^{PL}_{1992a} >= 2.98 \pm 0.06$, is inconsistently larger than that determined for the observations in June 1993, $< \Gamma^{PL}_{1993b} >= 2.78 \pm 0.09$. This inconsistency vanishes at a confidence level of only 90%. The mean photon index of the observations in Dec 1992 and Jan 1993, $< \Gamma^{PL}_{1992b,1993a} >= 2.92 \pm 0.12$ is consistent with that of the previous as well as of the following measurements. The derived N_H values are for all three observational epochs less than the Galactic value: $N^{PL}_{H\ 1992a} = (1.38 \pm 0.12) 10^{20}$ cm^{-2}, $N^{PL}_{H\ 1992b,1993a} = (1.20 \pm 0.20) 10^{20}$ cm^{-2}, and $N^{PL}_{H\ 1993b} = (1.18 \pm 0.17) 10^{20}$ cm^{-2}, respectively. This strength-

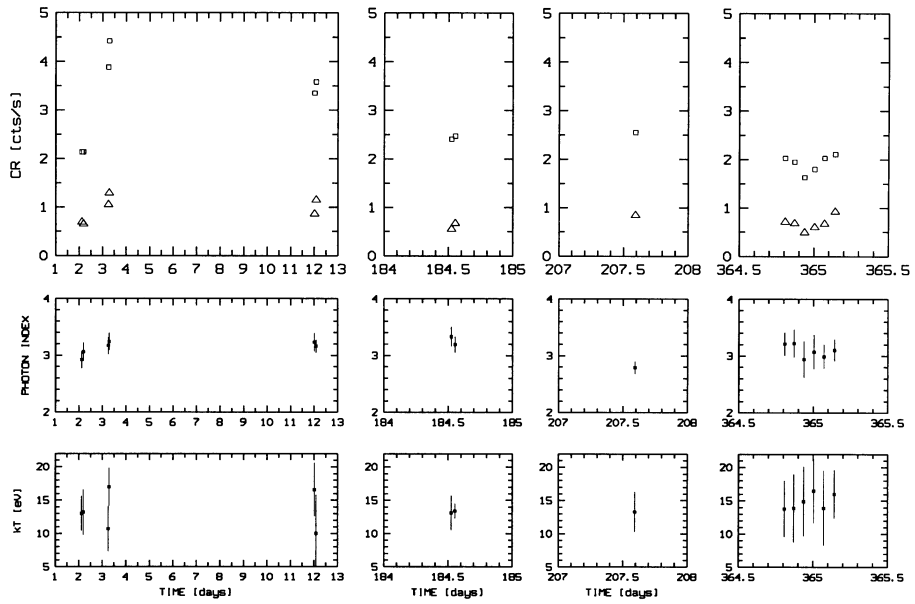

Fig. 8. Time dependence of the spectral parameters. Upper panel: Light curve at very soft X-rays (squares: (0.1 - 0.3)keV) and at harder X-rays (triangles: (0.5 - 2.4)keV). Middle panel: Power law photon index. Lower panel: Temperature of the black body component. The temporal structure of the diagrams is the same as in Fig. 4

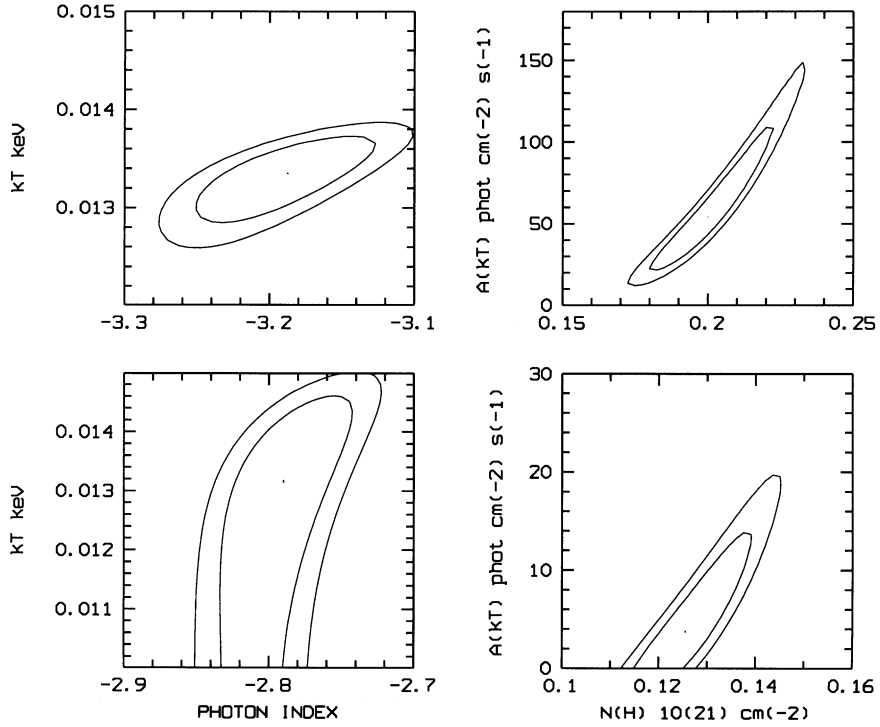

Fig. 9. Contour diagrams of the fit parameters of the low energy component. Upper panel: second orbit of the observation on Dec 18th, 1992. Lower panel: observation on Jan 10th, 1993. Left column: Black body temperature vs. power law index. Right column: Strength of the black body component vs. absorbing column density. The contours are given for two interesting parameters and for a 68.3% and a 90% confidence level, respectively.

ens also for the orbit spectra the conjecture that a realistic spectral model must be more complex than a simple power law.

Making use of the experience with the mean spectrum of the merged data set we choose as model spectrum a power law and a black body. N_H remains as a free fit parameter. The spectral parameters resulting from the fits of the two-component model to the orbit spectra are given in Table 2. In general, the adding of a very soft component to the power law continuum improves the fit of the orbit spectra in almost all cases with the one exception of the spectrum of orbit No.12, the residuals of which show unexplained systematic wiggles between 0.1 keV and 0.5 keV (see Fig. 10). From Table 2 it is obvious that the actual strength of the low energy component is not well constrained. However, the necessity of adding such a spectral component to the power law is certain: considering here only the June observations in 1992 and 1993, for which spectral variability is not obvious, and taking one standard deviation as uncertainty, the normalization of the black body is never consistent with omitting such an additional component. Only in the case of the less significant RASS observation is no additional component needed. The different behaviour of the quasar spectrum in late 1992 and in early 1993 will be discussed just below. The temperature (or steepness) of the low energy component is, however, well defined. Its mean value is kT = (14.0 $\pm$ 4.1) eV and the

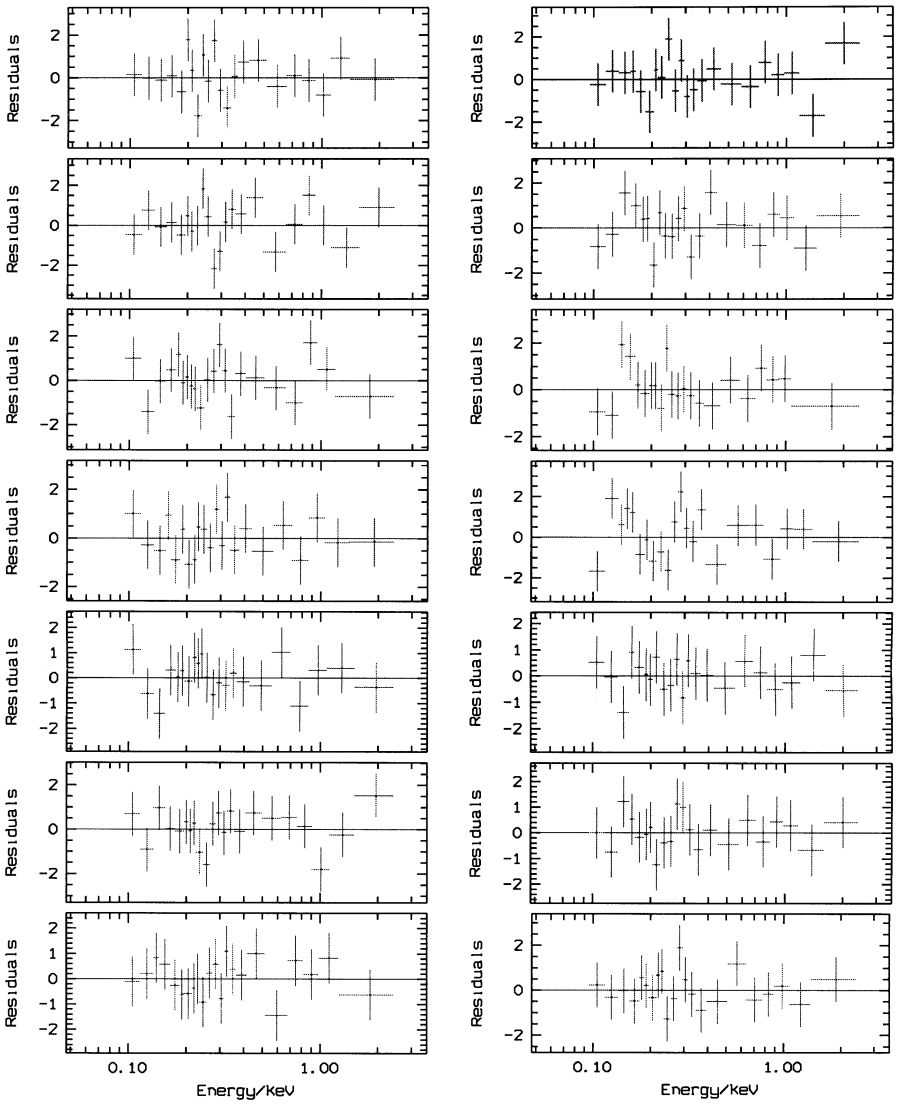

Fig. 10. Residuals of two-component model fits to the orbit spectra. Left column, top to bottom: Orbit No.1 to No.6, No.8 ; right column, top to bottom: Orbit No.9 to No.15

corresponding average temperatures for 1992 and for 1993 are consistent with each other. The photon index has a mean value of 3.12 ± 0.12 for the observational epochs in June 1992 and 1993: ($< \Gamma^{\rm PL+BB}_{\rm 1992a} >= 3.13 \pm 0.09$; $< \Gamma^{\rm PL+BB}_{\rm 1993b} >= 3.10 \pm 0.15$). These photon indices as well as the black body temperature of the orbit spectra are consistent with those values determined from the fit of the merged mean spectrum. Neither the temperature nor the index varies significantly for observations as can be seen from Fig. 8.

For the pointed observations in June 1992 an averaged N_H-value of $(2.32 \pm 0.46)10^{20}$ cm^{-2} was determined, whereas in June 1993 the average value amounts to $(3.30 \pm 0.80)10^{20}$ cm^{-2}. At a significance level of 68.3% these mean values are consistent with each other, but only the 1992 mean value is consistent with the N_H derived for the mean spectrum. Anyway, both averaged N_H-values are significantly larger than the Galactic value.

4.2.1. Spectral variability

In this section we consider only those observations which took place on Dec 18th, 1992, and on Jan 10th, 1993, respectively. During the two adjacent orbits in December the spectrum of the QSO was as steep as during previous epochs: $< \Gamma_{\rm 1992b} >= 3.26 \pm 0.16$. 23 days later the spectrum has become unusually flat, $\Gamma_{\rm 1993a} = 2.79 \pm 0.11$, - flatter than ever before and after. Together with a slight increase of the total count rate the flattening of the spectrum is accompanied by an increase of the normalization of the power law component at 1 keV. Fitting the spectra for normalizations at several photon energies in ROSAT's energy range shows that the change of the power law component between Dec 18 1992 and Jan 10 1993 is a rotation around a crossover point situated between 0.5 keV and 0.7 keV. Thereby the flux due to the power law component increased slightly by 16 per cent. The simultaneous behaviour of the low energy component is remarkable: while the characteristic parameters of the black body, temperature and strength, are positive definite even at a 90% confidence level during the December observations, the fit of the spectrum measured in January revealed that the same parameters are consistent with zero already at a confidence level of less than 68.3%. This situation is shown in Fig. 9. Using the best fit parameters the flux of the black body component de-

creased by about a factor of four between Dec 18, 1992, and Jan 10, 1993. Therefore we conclude that there are epochs at which the quasar shows spectral variability without a noticeable change of the total soft X-ray emission. Simultaneously with a flattening of the power law component, the component, usually dominant at very soft photon energies, vanishes. To date, such a behaviour of a soft X-ray excess has only been observed in the X-ray spectra of Seyfert 1 galaxies (e.g. NGC4051: Pounds et al. (1994), Komossa et al. (1996)).

4.2.2. Warm absorber?

Although the entirety of the residuals of the fit of a two-component model to the mean spectrum is in accordance with the expected statistical distribution, it is noticeable that there are low bins just around 0.7 keV and beyond 1 keV (Fig.5b). This could lead to the suspicion that these negative deviations from the model are caused by the effects of a warm absorber on the line of sight as has been found for several Seyfert galaxies, but not yet for QSOs (Nandra & Pounds, 1992; Ptak et al., 1994; Mihara et al., 1995). We checked the residuals of the fits of all orbit spectra (Fig.10). In the individual sequences we could not detect any systematic trend of low bins around 0.7 keV, where possible absorption edges of highly ionized oxygen should be located and should be visible for all physical conditions of a warm absorber with cosmic abundances. Therefore, we conclude that the ROSAT spectra do not indicate the existence of absorbing ionized material close to the nucleus of Ton S180.

5. Summary and conclusions

Close to the well defined optical position of the QSO Ton S180 ROSAT discovered the bright and soft X-ray source RX J0057.3–2222 during the all-sky survey in December, 1990. There were pointed follow-up observations of the X-ray source at four occasions in 1992 and 1993. The optical image of the QSO is well contained in the 90% error circle of the centroid of the X-ray point source image, so that an identification of RX J0057.3–2222 with the optical QSO is highly probable.

A study of the temporal behaviour of the X-ray emission of RX J0057.3–2222 in ROSAT's (0.1 - 2.4)keV energy band revealed intensity as well as spectral variability. Since the observations took place in three different years, each time for several but not always successive orbits, a temporal analysis of the observed X-ray emission cannot be undertaken on a continous grid of time scales. The limited time structure of the observations allows only to study the intra-orbit variability with a shortest time scale of 400s, the orbit-to-orbit variability where observations extend over adjacent orbits, and the long-term year-to-year variations. Nevertheless, it can be stated that Ton S180 shows a great variety of variability in its soft X-ray emission. The long-term variability on a time scale of years, which we observed with no indications of spectral changes, shows amplitudes up to a factor of two. On the other hand, the amplitudes usually found for the orbit-to-orbit variability ($\tau \approx 1.5$ h) do not exceed 30 per cent, a level which is also measured for the intra-orbit intensity variations ($\tau \approx 1200$ s). Generally, the latter variations are smooth. No "noisy" orbits were found as in the case of BL Lac objects.

Now and then Ton S180 shows outbursts like that measured during the pointed observations in June 1992. The X-ray emission rose from the actual persistent level of about 3.3 cts/s by more than a factor of two within less than a day. Although the ROSAT measurements show rather extended gaps, it looks as though the top level of the outburst might decay on a much longer time scale than that of the outburst's rise. Again, no indications of a spectral change accompanying the intensity jump could be found.

The investigation of the quasar's variable X-ray emission revealed that most of the time the spectrum is unchanged even in the case of strong intensity variations. In order to investigate the mean characteristics of the quasar's soft X-ray spectrum during those time intervals we merged the data sets of the pointed observations which were performed in June 1992 and one year later. These data do show intensity variations but no clear spectral variability. The mean spectrum is well represented by a two-component model consisting of a power law and a steep low energy component dominant below 0.3 keV. The influence of the low energy absorption (Galactic value $N_{Hgal} = 1.48 \cdot 10^{20}$ cm^{-2}, Stark et al., 1992) on this component of the intrinsic continuum prevents the exact determination of its spectral shape. We represented it by a black body spectrum, but it should be noted that another choice of model spectra like a second steeper power law or thermal bremsstrahlung does not change the goodness of the fit. The mean photon index of the power law component yielded by fitting the two-component model to the merged count rate spectrum is rather steep, $< \Gamma >= 3.10 \pm 0.05$, whereas the temperature of the black body is unusually low, $<$ kT $>= 15.7 \pm 2.5$ eV, thus demonstrating that this component is dominant only at very soft photon energies. Estimating the flux of the X-ray source in the (0.1 - 2.4)keV band on the basis of the two-component model for the continuum, we obtained an unabsorbed mean flux of $2.6 \cdot 10^{-10}$ erg cm^{-2} s which yield a soft X-ray luminosity of $\log L_X(0.1-2.4)$keV = 45.675 for a redshift of z = 0.06198 (H_o = 50 km/s Mpc ; q_o = 0).

Despite superb photon statistics of the mean spectrum, the strength of the steep low energy component remains more or less undefined. It is, therefore, difficult to compare the ROSAT (0.1 -2.4)keV flux with the (0.07 - 0.21)keV EUVE flux which has to be derived from the measured count rate of 0.053 cts/s by adopting a model spectrum for the continuum. The EUVE/Lexan energy range covers almost exactly that part of the spectrum, which is most affected by the cold matter absorption in our Galaxy, and where a possible steep component begins to dominate the power law continuum. Assuming the continuum to be represented by a power law only, Vennes et al. (1995) estimated a monochromatic flux density of $\nu F_\nu = 3.9 \cdot 10^{-11}$ erg cm^{-2} s at $\nu = 3.4 \cdot 10^{16}$ Hz (or E_o = 0.14 keV) adopting a photon index of Γ = 2.4 and an $N_H = 1.6 \cdot 10^{20}$ cm^{-2}. With our fit parameters we derive from the mean X-ray spectrum the ROSAT flux density of $\nu F_\nu{}^{PL+BB} = 2.1 \cdot 10^{-10}$ erg cm^{-2} s at 0.14 keV. This value is more than a factor of five larger than the reported monochromatic EUVE flux, but it should be kept in mind that

both observers adopted different slopes and absorbing column densities to reduce their flux densities. These different choices do not allow us to compare the reported EUVE flux directly with that one measured with ROSAT. Due to the exponential effect of the absorbing column density on the measured flux below 0.2 keV we speculate that the quasar's emission at very soft X-rays was clearly weaker at the time of the EUVE measurement than during the pointed observations with ROSAT.

The detailed study of the parameters of individual orbit spectra confirms that there are spectral variations neither of the power law continuum nor of the black body component for the data measured in mid 1992 and one year later. On the other hand, a clear change of the quasar's spectrum can be stated for the time interval between the observation on Dec 18, 1992, and the measurement performed 23 days later in Jan, 1993. In Dec 1992 the power law component of the spectrum is steep ($\Gamma \approx 3.26$) and the low energy component is definitely existent. Twenty three days later the power law component has become flatter ($\Gamma = 2.79$) without a noticeable change of its flux contribution. This component looks as though it is rotated relative to the steeper spectrum measured in Dec 1992 around a crossover point near 0.6 keV. Simultaneously with the flattened power law component we find the black body component weakened by at least a factor of four in Jan 1993. In fact, the strength as well as the temperature of this component is consistent with zero for this observation. The relative change in the total flux within (0.1 - 2.4)keV accompanying the spectral variation is only about 10 per cent. Half a year later all spectral parameters are back again to the values measured a year before and during the all-sky survey.

By inspecting the residuals of all orbit spectra it can be excluded that the ROSAT spectra show any sign of a warm absorber on the line of sight.

As mentioned above, Ton S180 is a narrow line QSO (H_β(FWHM) = 900 km/s, Wisotzki et al. (1995)) with an optical Seyfert 1 spectrum. Also its soft X-ray properties go with those of the class of narrow line Seyfert 1 galaxies (NLSY1): with its characteristic parameters $[\Gamma, H_\beta(\mathrm{FWHM})] = [3.10, 900]$ the QSO belongs well to the domain of NLSY1s in Fig. 8 of Boller, Brandt, and Fink (1995) which shows that NLSY1s usually have steeper soft X-ray spectra than broad-line Seyfert 1 galaxies. A second feature of NLSY1s is their X-ray variability, the doubling time of which ranges from 800 s to several hours. The formal doubling time of the intra-orbit variations of Ton S180 was measured to be about 2 hours, whereas for the doubling time of the outburst's rise only an upper limit of one day could be given due to an observational gap of 15 orbits. Therefore, as far as the time scales of the observed variability are concerned, the QSO Ton S180 behaves like a NLSY1. To date, the medium energy spectrum of Ton S180 above 2 keV has not been measured. Only for one of the brightest NLSY1 galaxies, RE 1034+39, discovered with the ROSAT Wide Field Camera (Pounds, 1994), a measurement of the medium energy spectrum with the detectors aboard the ASCA satellite was reported (Pounds, Done, and Osborne, 1995). Surprisingly, the source shows a steep (2 - 10)keV power law spectrum with a photon index of $\Gamma \sim 2.6$. It will be of high interest to see whether such steep hard X-ray spectra are a class property of NLSY1s, and whether narrow line QSOs like Ton S180 behave analogously.

Acknowledgements. The ROSAT mission was supported by the Ministerium für Forschung und Technologie (BMFT, Deutschland) and by the Max-Planck-Gesellschaft. We would like to thank the ROSAT team for processing the observational data. We thank the referee, Dr. N. Jackson, for his advice. We are grateful to be able to make use of the photographic data obtained using The UK Schmidt Telescope, which was operated by the Royal Observatory, Edinburgh, with funding from the UK Science and Engineering Research Council and from Anglo-Australian Observatory. The Digitized Sky Survey was produced at the Space Telescope Science Institute under US Government grant NAG W-2166.

References

Aschenbach B., 1988, Appl.Optics **27**, 14
Boller Th., Brandt W.N., Fink H., 1995, A& A, in press
Bowen D.V., Osmer S.J., Blades J.C., et al., 1994, AJ **107**, 461
Bowyer S., Lieu R., Lampton M., et al., 1994, ApJS **93**, 569
Briel U.G., 1991. Internal ROSAT Memorandum, Oct.28
Brinkmann W., Maraschi L., Treves A., et al., 1994, A& A **288**, 433
Chavira E., 1958, Bol. Obs. Tonantzintla Tacubaya **2** No.17, 15
Hamuy M., Maza J., 1987, A& AS **68**, 383; 1989, AJ **97**, 720
Komossa S., et al., 1996, in preparation
Kondo M., Noguchi T., Maehara H., 1984, Ann. Tokyo Astron. Obs. **20**, 130
Mihara T., Matsuoka M., Mushotzky R., et al., 1995, PASJ **46**, L137
Nandra K., Pounds K.A., 1992, Nature **359**, 215
Pfeffermann, E., Briel, U.G., Hippmann, H., Kettenring, G., Metzner, G., Predehl, P., Reger, G., Stephan, K.-H., 1987, MPE print **81**
Pounds K.A., Done C., Osborne J.P., 1995, MNRAS 277, L5
Pounds K.A.,1994, X-ray spectroscopy of active galactic nuclei 1980-2000. In: Makino F., Ohashi T. (eds.)New Horizon of X-ray Astronomy. Universal Academic Press Inc., Tokyo, p.293
Pounds K.A., Nandra K., Fink H.H., Makino F., 1994, MNRAS **267**, 193
Ptak A., Yaqoob T., Serlemitsos P.J., Mushotzky R., Otani C., 1994, ApJ **436**, L31
Schmidt M., Green R.F., 1986, ApJ **269**, 352
Stark A.A., Gammie C.F., Wilson R.W., et al., 1992, ApJS **78**, 77
Thomas H.-C., Beuermann K., Brinkmann W., Fink H.H., Voges W., 1991, Spectroscopic identification of X-ray soft AGN found by ROSAT. In: Brinkmann W., Trümper J. (eds.) X-ray emission from active galactic nuclei and the cosmic X-ray background, MPE Rep. 235, p.383
Trümper, J., 1983, Adv. Space Res. **4**, 241
Vennes S., Polomski E., Bowyer S., Thorstensen J.R., 1995, ApJ **448**, L9
Veròn-Cetty M.-P., 1984, A& AS **58**, 665
Voges W., 1992, The ROSAT All-Sky X-Ray Survey. In: Guyenne T.D., Hunt J.J. (eds.) Spaces Science with particular emphasis on High-Energy Astrophysics. ESA ISY-3, 9
Walter R., Fink H.H., 1993, A& A **274**, 105
Walter R., Orr A., Courvoisier T.J.-L., et al., 1994, A& A **285**, 119
Winkler H., 1992, MNRAS **257**, 677
Wisotzki L., Dreizler S., Engels D., Fink H.H., Heber U., 1995, A& A **297**, L55